Journal Pre-proof

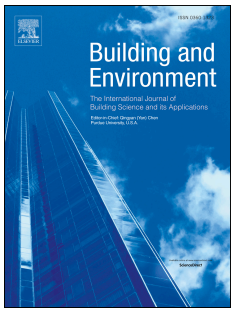

A 3D multi-segment thermoregulation model of the hand with realistic anatomy: Development, validation, and parametric analysis

Mengying Zhang, Rui Li, Jun Li, Faming Wang, Shankar Subramaniam, James Lang, Alberto Passalacqua, Guowen Song

PII: S0360-1323(21)00368-1

DOI: https://doi.org/10.1016/j.buildenv.2021.107964

Reference: BAE 107964

To appear in: *Building and Environment*

Received Date: 28 March 2021

Revised Date: 28 April 2021

Accepted Date: 12 May 2021

Please cite this article as: Zhang M, Li R, Li J, Wang F, Subramaniam S, Lang J, Passalacqua A, Song G, A 3D multi-segment thermoregulation model of the hand with realistic anatomy: Development, validation, and parametric analysis, *Building and Environment* (2021), doi: https://doi.org/10.1016/j.buildenv.2021.107964.

A 3D multi-segment thermoregulation model of the hand with realistic anatomy: development, validation, and parametric analysis

Mengying Zhang [a, b], Rui Li [a], Jun Li [b,c], Faming Wang [d], Shankar Subramaniam [a], James Lang [a], Alberto Passalacqua [a], Guowen Song [a, *]

[a] Iowa State University, Ames, Iowa, 50010, USA.

[b] College of Fashion and Design, Donghua University, Shanghai, 200051, China.

[c] Key Laboratory of Clothing Design and Technology, Donghua University, Ministry of Education, Shanghai, 200051, China.

[d] Central South University, Changsha, Hunan, 410011, China.

Abstract

A three-dimensional (3D) multi-segment hand-specific thermoregulation model was developed as a fundamental tool for spatial and temporal skin temperature prediction. Cold-induced vasodilation in fingers was simulated by superimposing symmetrical triangular waveforms onto the basal blood flow. The model used realistic anatomical, physiological, and thermo-physical information of a standard human hand and forearm. The inhomogeneity of hand thermal and physiological properties was considered by dividing it into 17 segments: palm, dorsal, forearm, and five fingers, with each finger subdivided into fingertip, middle segment, and finger root except for the thumb, which has no middle segment. Each segment contained a bone core and an outer soft tissue layer. 3D scanning technology was employed to develop the geometrically realistic model of the hand and the bone. The thermo-physical and physiological properties of each segment and layer were obtained from a photogrammetric analysis of anatomic atlases and from literature. Heat transfer throughout the hand by metabolism, blood perfusion, and conduction between the tissue was considered. Heat loss by convection and radiation from the skin and the protective effects of gloves were also included in the model. The model showed good agreement with experimental data from the literature. The developed 3D hand model fills the knowledge gap and builds a bridge between existing knowledge of the hand's physiology and its application, providing a science-based tool for decision making. The understanding from model studies may also help enhance the wearer's working efficiency, safety, health, and wellbeing while working in indoor and outdoor cold environments.

Keywords: human hand, finger, thermoregulation model, skin temperature, cold stress, CIVD

1 Introduction

Cold environments pose a significant threat to human comfort, work efficiency, and safety. The incidence of accidents rises extraordinarily while working in the cold outdoor and indoor environments, such as in a cold windy or in an unheated building in the winter. It is reported that more than 500,000 occupants have suffered from cold injury in their work environments in Finland [1]. Specifically, building construction workers suffer from cold weather injuries severely. One of the reasons to cause the accidents in the cold environment is the numbness of the human hand. Besides, even local hand exposure in the cold environmental can intensify the discomfort of the whole human body [2].

Human hands are unique, extremely dexterous, and play a critical role in human activities. Hand and finger skin temperatures are pivotal factors to maintain dexterity, grip strength, and manual performance [3, 4]. Laboratory and field studies have shown that performing the same type of manual work in a cold environment is more dangerous than in a warm environment [1]. A mean hand skin temperature of 15 ℃ is considered to be the lowest acceptable temperature for maintaining sufficient hand manual performance [3, 5]. Finger dexterity is more sensitive to cold exposure than manual dexterity [6]. Finger dexterity weakens slightly at a finger skin temperature of 20-22 ℃, and severe finger dexterity deterioration is often seen at a finger skin temperature of 15-16 ℃, which substantially increases the risk of accidents while working [7-9]. Almost all subtle functions of the fingers are lost when the finger temperature drops to 4.4 ℃ [10]. The number of errors (when performing a tracking task) increases approximately linearly with the decreasing hand temperature within the ambient temperature range of 10-30 ℃ [11]. Dexterity and grip strength are also positively correlated with finger skin temperatures [12]. Impairment of manual performance during cold exposure is also dependent on many other factors such as the ambient air temperature, glove material properties (e.g., thickness and stiffness), and glove design factors [12, 13]. It is important to keep the skin temperatures above a certain threshold to maintain hand performance and reduce the risk of accidents.

Hands are also rather effective at losing heat to the environment due to the considerable and frequent changes in blood flow and a rather large surface-to-volume ratio that is 4 to 5 times larger than the body as a whole [14, 15]. In general, the blood flow in the hand can be as low as 0.15 ml/100 ml tissue/min during prolonged cold exposure [16], and, during high-temperature exposure, it can reach up to 30 ml/100ml tissue/min [17], i.e., a 200-fold difference. Nagasaka et al. [18] reported that the minimal blood flow in fingers was 0.2 ml/100ml tissue/min, while the maximum could reach as high as 120 ml/100 ml tissue/min in locally heated hands. The 600-fold changes in blood flow through the fingers are unparalleled in any other part of the hand. Moreover, for any given finger, the blood flow in the fingertip can be three times larger than that in the finger's middle segment [19]. Additionally, a larger surface-to-volume ratio will result in a high-

er heat exchange rate, making hands, especially fingers, more susceptible to heat loss in cold environments than other parts of the body.

During cold exposure, vasoconstriction in the skin decreases the peripheral blood flow so that convective heat transfer between the body core and shell could be decreased. However, peripheral constriction results in strong cooling of extremities. Fortunately, extremities such as the hand have the capability to prevent the occurrence of cold extremities. After the initial exposure of the hand to cold for about 5-10 minutes, blood vessels in the fingertips suddenly vasodilate. Subsequently, the peripheral blood flow and the temperature of the fingertips increase. This phenomenon is called *cold-induced vasodilation* (CIVD). CIVD appears to occur when the finger skin temperature drops to a range of 7.2-18 ℃ depending on many factors such as thermal state, ethnicity, gender, age, fitness, alcohol, tobacco, diet, adaptation, and acclimation [20, 21]. CIVD could last for a few minutes and is flowed by a phase of vasoconstriction. Once the finger skin temperature decreases to the above-mentioned threshold temperature range, another burst CIVD may occur [21]. This process repeats itself and is called *the hunting reaction* [21]. CIVD can likely mitigate cold injuries and maintain manual dexterity for longer durations [22, 23].

A mathematical model of hand thermoregulation in cold environments provides an efficient, safe, and economical method to predict the evolution of skin temperatures of the hand and fingers and reveal the thermal interaction between the human hand and the environment. Transient one-dimensional models of the hand-object thermal interaction have been developed to simulate skin temperature change and predict skin injuries [24-26]. They require the initial skin and object temperatures, skin thermal conductivity and diffusivity, and contact conductance as input parameters. Nevertheless, those models are unable to simulate hand thermoregulation through processes such as vasomotion, which greatly limits their predictive capabilities.

Advanced models that consider thermoregulation and account for clothing and other environmental factors have been developed [27, 28]. However, most of the existing thermoregulation models either simplify the hand geometry as a cylinder [29-32] or only focus on a single finger [33-37]. While whole-hand models typically neglect any differences in thermal responses between the palm, dorsal, and especially individual fingers (caused by different anatomies, geometries, and physiological and thermo-physical characteristics), single-finger models fail to account for and differentiate thermal responses of other hand regions. There is a limited number of existing models that address differences in physiological responses [38] between hands and fingers or realistic dimensions of the hand [39]. The anatomical heterogeneity and the diverse geometry of the hand, which significantly affects the heat transfer coefficients [40] and the hand temperature profiles [41], are not usually taken into consideration in both whole hand and single finger models. Failure to simulate local differences in the thermo-physiological hand response makes it impossible to accurately predict temperatures of all fingers, present a temperature profile of the entire hand, as well as provide essential information for hand protection [42]. To date,

there exists no hand thermoregulation model that considers both the realistic geometry and the inhomogeneity of the hand and fingers to predict the temperature distribution and changes over time. In order to bridge the gap and facilitate the formulation of effective strategies for maintaining good dexterity and reducing the risk of cold injuries, it is crucial to develop a hand-specific thermoregulation model that is capable of simulating the thermophysiological responses of both the whole hand and of the different segments with sufficient accuracy.

To achieve this goal, we developed a 3D multi-segment hand-specific thermoregulation model that uses a more realistic representation of the hand and its skeletal anatomy and geometry based on 3D scanning techniques. Hand heterogeneity is addressed by dividing the virtual hand model into 17 segments, namely the forearm, palm, dorsal, and five fingers, with each finger subdivided into fingertip, middle segment, and finger root, except for the thumb, which has no middle segment. Each segment consists of two layers: a bone core that is surrounded by an outer soft tissue layer. The physiological and thermo-physical properties of each segment and each layer have been obtained from a photogrammetric analysis of anatomic atlases. The model can account for heat transfers due to metabolism, blood perfusion, and conduction between each segment and layer. Vasoconstriction is simulated by describing the blood flow as a function of body core temperature, average body skin temperature, and local hand temperature. CIVD is simulated by superimposing symmetrical triangular waveforms on the basal blood flow rate. Heat losses from the skin surface by convection and radiation are also considered. The effect of gloves is simulated by adding an additional layer of thermal insulation on top of the hand's skin layer. Skin temperature changes over time for a range of air temperatures and wind speeds were successfully predicted and validated against literature data (with and without CIVD/gloves). The effect of wind speeds and air temperature on spatial distribution and temporal dynamics of hand skin temperature were analyzed.

2 Method

2.1 Geometrical model

The numerical hand model was divided into two layers: the outer soft tissue and the bone core. The soft tissue layer contains skin, muscle, and fat. The hand geometry was obtained from a 3D scan of a thermal hand manikin (Thermetrics, Seattle, WA) and represents a standard human hand (50 percentile western male hand size). The bone geometry used is a simplified version of the hand skeleton. The geometry of the hand skeleton was digitized via 3D scanning of an anatomically correct model (Axis Scientific, Evanston, IL). However, the geometry of the skeleton, especially of the carpal bones, is quite complex and contains a certain degree of irregularity. Hence, this requires many mesh control volumes to be adequately resolved, which lead to an in-

creased computational cost (Fig. 1a). Therefore, the geometry of the skeleton was approximated as smooth curved surfaces and using the Geomagic Studio 12 software (3D Systems, Inc., USA). The positions and postures of fingers were adjusted to fit the virtual hand model using ICEM CFD 2020 R2 (Ansys Inc., Canonsburg, PA, USA) (Fig. 1b). The relative location between the virtual hand and bone model was adjusted in order to make the thickness of the soft tissue at the left and right side of the finger is equal and at the palmar and the dorsal side of the finger is about 2.39:1 and 1.52:1 for the thumb and the other four fingers, respectively [31] (Fig. 1c). The distance between the tip of the soft tissue and the bone of the finger was adjusted to about 4.9 to 5.0 mm [43]. The forearm bone was digitally generated and simplified by shrinking its geometry while maintaining a 6.0 mm soft tissue thickness [44]. The coupled hand and bone model was then divided into 17 segments (Fig. 1d). The volume percentage of the bone in the hand model ranged from about 15% to 23%, 19% to 25%, and 23% to 28%, in the fingertips, middle segments, and finger roots, respectively, or was a constant of 15%, 24%, and 26% in the palm, dorsal, and forearm, respectively.

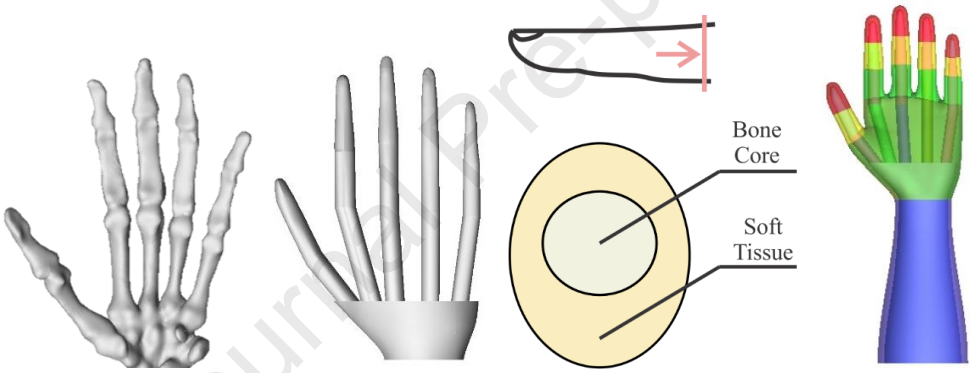

Fig. 1. Hand anatomy used in the model. (a) the real hand bone model, (b) simplified hand bone model, (c) a cross-sectional view of one finger to illustrate the bone core and soft tissue layer., and (d) the coupled hand and bone model with 17 hand segments.

A tetrahedral volume mesh was created for the 3D hand domain using ICEM CFD 2020 R2 (Ansys Inc., Canonsburg, PA, USA). A grid independence study was conducted focusing on the skin temperature as this is the critical and most sensitive parameter (rather than bone or tissue temperature) with regard to the number of mesh elements. We eventually chose a total number of about 1.16 million mesh nodes for the simulation as a further increase to 2.50 million only resulted in negligible changes (of less than 0.01%) in the surface temperature of all 17 segments.

2.2 Heat transfer model

In this study, the change in tissue temperature is described as a sum of conductive heat transfer within the tissue, heat generation by blood flow, and metabolic heat generation:

$$\rho c_p \frac{\partial T}{\partial t} = \frac{\partial}{\partial x}\left(k\frac{\partial T}{\partial x}\right) + \frac{\partial}{\partial y}\left(k\frac{\partial T}{\partial y}\right) + \frac{\partial}{\partial z}\left(k\frac{\partial T}{\partial z}\right) + q_b + q_m \quad \text{Eq. 1}$$

where ρ (kg/m^3), c_p (J/(kg·K)), and k (W/(m·K)) are the density, specific heat capacity, and thermal conductivity of the hand tissue, respectively, T (K) is the tissue temperature, t (s) is time, q_b (W/m^3) and q_m (W/m^3) are the heat generated by blood flow and basal metabolism, respectively. Although shivering is a vital response to generate heat when the human body is exposed to a cold environment, it contributes only little to the hand thermal response due to a very limited percentage of muscle in the hand [45]; therefore, shivering was neglected in this model.

2.2.1 Tissue properties

There is very little existing knowledge regarding the thermo-physical properties of the soft tissues in each hand segment. In this research, the density, specific heat, thermal conductivity, and metabolic heat generation of each hand segment were derived based on the following approaches and underlying assumptions.

2.2.1.1 Volume percentages of muscle, fat, and skin in each segment

The volume percentages of muscle, fat, and skin in the soft tissue for each segment of the finger were estimated from Yuan [46], who simplified the finger as a cylindroid, and provided seven cross-sections along the major and minor axis showing the proportions of bone, muscle, fat, and skin from the finger root to the fingertip. We used Yuan's data to calculate the cross-sectional areas at the bottom of the finger root, at the proximal and distal and interphalangeal joints, and at the top of the fingertip. The fingertip, middle segment, and finger root were each considered as truncated cones when calculating the volume percentages, and the corresponding volume can be calculated from ([47]):

$$V = h\left(a + b + \sqrt{ab}\right)/3 \quad \text{Eq. 2}$$

where V (m^3) is the segmental volume, h (m) is the distance between adjacent cross-sections, and a (m^2) and b (m^2) are the respective top and bottom cross-sectional areas of each segment. Furthermore, we assumed that the volume percentages of muscle, fat, and skin did not differ between fingers.

The volume percentages of muscle, fat, and skin in the palm and dorsal soft tissue were estimated from Dixon et al. [48] (Fig. 2). The area percentages of the muscle, fat, and skin were estimated by using AutoCAD 2016 software (Autodesk Inc., USA) based on the cross-section image shown in Fig. 2. It was assumed the area percentage of soft tissue components is the same along the length of palm and dorsal, thus representing the volume percentage in this study.

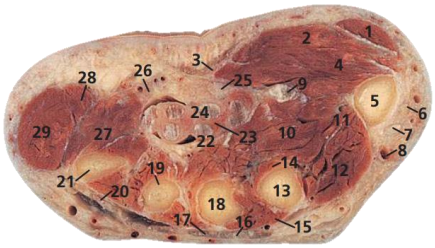

1 Abductor pollicis brevis
2 Flexor pollicis brevis
3 Palmar aponeurosis
4 Oponens pollicis brevis
5 First metacarpal
6 Extensor pollicis brevis tendon
7 Extensor pollicis longus tendon
8 Cephalic vein
9 Flexor pollicis longus tendon
10 Adductor pollicis
11 Radial artery
12 First dorsal interosseous
13 Second metacarpal
14 Second palmar interosseous
15 Second dorsal interosseous
16 Extensor indicis tendon
17 Extensor digitorum tendon
18 Third metacarpal
19 Fourth metacarpal
20 Extensor digiti minimi tendon
21 Fifth metacarpal
22 Flexor digitorum profundus tendons
23 Lumbrical
24 Flexor digitorum superficialis tendons
25 Median nerve
26 Ulnar artery and nerve
27 Opponens digiti minimi
28 Flexor digiti minimi
29 Abductor digiti minimi
30 Muscles of thenar eminence
31 Muscles of hypothenar eminence

Fig. 2. Anatomical cross-section through the proximal shafts of the hand's metacarpals.

The volume percentages of muscle, fat, and skin in the forearm were taken from Cooper et al. [49] who obtained the data from measurements on dissected cadavers. Table 1 provides a summary of all volume percentages used in this study.

Table 1. Volume parentages of muscle, fat, and skin in the soft tissue of different hand segments used in the present study.

	Muscle	Fat	Skin
Fingertip	23.79%	61.00%	15.21%
Middle segment	39.62%	45.91%	14.47%
Finger root	43.77%	41.77%	14.46%
Palm	73.18%	16.50%	10.32%
Dorsal	36.17%	36.86%	26.97%
Forearm	80.76%	9.27%	9.97%

2.2.1.2 Thermo-physical and physiological properties of each segment

The thermo-physical and physiological properties of the soft tissue were calculated based on a volume-weighted average (Eq. 3 to Eq. 6) of the corresponding properties of each constituent, i.e., muscle, fat, and skin. The individual values of the muscle, fat, and skin were taken from Fiala et al. [30] and Shitzer et al. [37] (Table 2).

Table 2. Density, specific heat, thermal conductivity, and basal metabolic rate of the different soft tissue constituents used to calculate their volume averages for use in the numerical computations [30, 37].

	Density (kg/m^3)	Specific heat ($J/(kg \cdot K)$)	Thermal conductivity ($W/(m \cdot K)$)	Basal metabolic rate (W/m^3)
Muscle	1085	3768	0.42	684

Fat	850	2300	0.16	58
Skin	1085	3680	0.47	368

$$\rho_{soft\_tissue} = v_{muscle}\rho_{muscle} + v_{fat}\rho_{fat} + v_{skin}\rho_{skin} \quad \text{Eq. 3}$$

$$c_{p_{soft\ tissue}} = v_{muscle}c_{p_{muscle}} + v_{fat}c_{p_{fat}} + v_{skin}c_{p_{skin}} \quad \text{Eq. 4}$$

$$k_{soft\ tissue} = v_{muscle}k_{muscle} + v_{fat}k_{fat} + v_{skin}k_{skin} \quad \text{Eq. 5}$$

$$M_{soft\ tissue} = v_{muscle}M_{muscle} + v_{fat}k_{fat} + v_{skin}M_{skin} \quad \text{Eq. 6}$$

where ρ (kg/m^3), c_p(J/(kg·K)), k(W/(m·K)), and M (W/m^3) are the density, specific heat, thermal conductivity, and basal metabolic rate, respectively; the subscripts $soft\_tissue$, $muscle$, fat, and $skin$ refer to the soft tissue, muscle, fat, and the skin, respectively.

The density, specific heat, thermal conductivity, and basal metabolic rate of the soft tissue in each hand segment were obtained and are summarized in Table 3. Additionally, the properties of the bone and blood used in this study are listed in Table 4.

Table 3. Density, specific heat, thermal conductivity, and basal metabolic rate for the soft tissue in different hand segments.

	Density (kg/m^3)	Specific heat (J/(kg·K))	Thermal conductivity (W/(m·K))	Basal metabolic rate (W/m^3)
Fingertip	942	2859	0.2690	254.1
Middle digit	977	3081	0.3079	350.9
Finger root	987	3142	0.3186	376.8
Palm	1046	3517	0.3823	548.1
Dorsal	998	3203	0.3376	368.0
Forearm	1063	3623	0.4009	594.5

Table 4. Density, specific heat, thermal conductivity, and basal metabolic rate for the bone and blood.

	Density (kg/m^3)	Specific heat (J/(kg·K))	Thermal conductivity (W/(m·K))	Basal metabolic rate (W/m^3)
Bone core	1357	1700	0.75	0
Blood	1060	3899	0.45	

2.2.2 Blood flow and heat transfer

The heat transfer by blood flow is calculated based on

$$q_b = \omega_b\rho_b c_{p_b}(T_{art} - T_{ven}) \quad \text{Eq. 7}$$

where ω_b (s^{-1}) is the blood flow rate per unit volume, ρ_b (kg/m^3) and c_{p_b} (J/(kg·K)) are the density and specific heat of the blood, and T_{art} (K) and T_{ven} (K) are the temperatures of the arterial and venous blood.

The whole hand was perfused with a basal blood flow and an arterio-venous shunt flow, and the local reaction to cold is a decrease in blood flow and thus in heat dissipation [50]. In this study, the blood flow rate is considered as a function of body core temperature, average skin temperature of the whole body, and local skin temperature [51]:

$$\omega_b = \omega_{basic} + exp\left(1.5\left((T_{core} - 309.95) + 0.15(\bar{T}_{skin} - 306.15) + 0.2(T - 302.15)\right)\right)/3000 \quad \text{Eq. 8}$$

where ω_{basic} (s^{-1}) is the basal blood flow assumed to be 5×10^{-5} s^{-1} [52], T_{core} (K) is the body core temperature, and $\bar{T}_{skin}$ (K) is the average skin temperature of the whole body.

During cold exposure, peripheral blood returns to the heart through deep veins to reduce heat loss and thereby cools the blood in adjacent arteries through a countercurrent heat exchange mechanism. Heat loss per unit volume of blood is an almost linear function of the hand skin temperature. The difference in temperature between arterial and venous blood as it enters and leaves the hand is about 8 K and 1.1 K for hand skin temperatures of 289.15 K and 309.15 K, respectively [16]. Therefore, we can establish a linear equation that describes the drop in blood temperature as a function of the hand skin temperature:

$$T_{art} - T_{ven} = -0.345T + 107.7568 \quad \text{Eq. 9}$$

2.2.2.1 Modeling cold-induced vasodilation (CIVD)

During cold exposure, vasoconstriction reduces blood flow and hence heat dissipation. However, when the skin temperature has dropped to 18 ℃ or lower [21, 53], a seemingly paradoxical cold-induced vasodilation (CIVD) occurs, most commonly in fingers and toes, temporarily increasing blood flow and leading to rewarming. During CIVD, the skin temperature may rise by as much as 10 ℃. As the temperature rises, vasoconstriction occurs again and causes the skin temperature to fall. This cycle may repeat many times [54]. Moreover, higher body core temperature will cause earlier onsets of CIVD which will result in higher finger skin temperatures during CIVD [21]. While CIVD has been hypothesized to protect against cold injury, the exact physiological mechanisms behind CIVD remain unclear. It appears that only a minority of humans possess the natural capability of CIVD, and there are large differences in the onset time, duration, and amplitude of CIVD among peoples [36, 55]. Therefore, we simulate CIVD by assuming that CIVD lasts for 5 min and is followed by 5 min of asymmetrical vasoconstriction [37]. The change in blood flow rate with time is shown in Eq. 10.

$$\omega_{b,CIVD} = \begin{cases} \omega_b + \omega_{peak}(t + 60 - t_{onset})/60\,, during\ the\ first\ 5\ min\ of\ CIVD \\ \omega_b + \omega_{peak}\big(660 - (t + 60 - t_{onset})\big)/60\,, during\ the\ last\ 5\ min\ of\ CIVD \end{cases} \quad \text{Eq. 10}$$

where ω_{peak} (s^{-1}) is the peak blood flow rate during CIVD and t_{onset} (s) is the onset time of CIVD.

Based on the above assumptions, the heat transfer by blood flow considering CIVD can then be calculated using Eq. 11.

$$q_b = \omega_{b,CIVD}\rho_b C_{p_b}(T_{art} - T_{ven}) \quad \text{Eq. 11}$$

2.3 Boundary and initial conditions

For model validation, the initial temperature of the soft tissue was set to the value of the skin temperature as measured in the experiment. The initial temperature of the bone core was assumed to be 34 ℃ [45].

Heat loss from the hand skin exposed to cold air occurs through convection and radiation. The convective heat loss from the skin is calculated by

$$q_c = h_c(T_{air} - T) \quad \text{Eq. 12}$$

where q_c (W/m^2) is the heat loss from the skin surface by convection, T_{air} (K) is the ambient air temperature, and h_c ($W/(m^2 \cdot K)$) is the convective heat transfer coefficient of the different hand segments. For wind speed range from 0.05 m/s to 2.0 m/s, h_c was determined by the regression equation, which has the general form:

$$h_c = au^n \quad \text{Eq. 13}$$

The corresponding values for a and n can be found in reference [40]. For wind speed larger than 2.0 m/s, h_c was determined by [53]

$$h_c = Nuk_{air}/L \quad \text{Eq. 14}$$

where k_{air} ($W/(m \cdot K)$) is the thermal conductivity of air, L (m) is the characteristic length (for a cylindrical representation of a finger, the finger diameter can be taken as the characteristic length), and Nu is the Nusselt number. For forced convection,

$$Nu = BRe^n \quad \text{Eq. 15}$$

where B and n are shape factors and, for a cylinder, can be estimated as $B = 0.24$ and $n = 0.60$, and Re is the Reynolds number and can be calculated from

$$Re = vL/\mu \quad \text{Eq. 16}$$

where v (m/s) is the wind speed and μ (m^2/s) the kinematic viscosity of air.

The radiative heat loss from the skin is given by

$$q_r = f\varepsilon\sigma(T^4 - T_r^4) \quad \text{Eq. 17}$$

where q_r (W/m^2) is the heat loss from the skin surface by radiation, f is the view factor of each hand segment (see Table 5) obtained based on a previous study [40], ε the emissivity of the skin

(a constant value of 0.95 is assumed in this study), σ the Stefan-Boltzmann constant (5.67×10^{-8} W/(m^2·K^4)), and T_r (K) the mean radiant temperature assumed to be equal to T_{air} [42].

Table 5. View factors for each hand segment.

Hand segment		View factor
Thumb	Fingertip	0.8797
	Finger root	0.8637
Index	Fingertip	0.8872
	Middle digit	0.8401
	Finger root	0.7994
Middle	Fingertip	0.8599
	Middle digit	0.7540
	Finger root	0.7055
Ring	Fingertip	0.8616
	Middle digit	0.7677
	Finger root	0.7320
Little	Fingertip	0.8635
	Middle digit	0.8429
	Finger root	0.8287
Palm		0.9313
Dorsal		0.9631
Forearm		0.9681

2.4 Numerical solution

ANSYS FLUENT (Ansys Inc., Canonsburg, PA, USA), and specifically the SIMPLEC algorithm, was used to solve the governing equations based on the finite volume method. A least-squares cell-based algorithm for gradients and a second-order upwind scheme for the energy equation were used for discretization. The solution was considered as converged when the residual level dropped to 1×10^{-7} for the energy equation. We also studied the dependence of the model results on the chosen time step. Changing the time step from 1 s to 0.1 s resulted in changes in the skin surface temperatures of all segments of well below 0.5%. We therefore chose a time step size of 1 s to balance numerical accuracy and computational cost.

3 Results and Discussion

The developed 3D hand thermoregulation model was validated using four different scenarios: two extreme cold scenarios which we will refer to as **Scenario 1** (-26 ℃ with 5 m/s wind) and **Scenario 2** (-15 ℃ with 10 m/s wind), a cold scenario which we label **Scenario 3** (0 ℃ with 0.4 m/s wind), and a slightly cool scenario labeled **Scenario 4** (14 ℃ with 1.5 m/s wind). The modeled results were compared with published experimental and simulation data. After validation, the model is used to investigate the effect of wind speed (0.05 m/s to 2.0 m/s) and air temperature (-10 ℃ to 10 ℃) on the spatial and temporal skin temperature distribution of the hand.

3.1 Model validation for Scenarios 1 and 2

The predicted change in skin temperature in the two extreme cold scenarios (Scenarios 1 and 2) is in good agreement with experimental data from Wilson and Goldman [56] (Fig. 3 and Fig. 4) in which an air temperature as low as -26 ℃ was simulated. In their experiment, the middle segment of an unspecified finger was inserted into a temperature-controlled chamber (16 cm ×8 cm × 3 cm) where a jet of cold air was directed at the finger segment's dorsal surface. The air velocity was measured at the site of the finger by an air velocity meter. Meanwhile, other hand segments and body parts were exposed to an ambient air temperature of 21 ℃ while the torso and lower body of the test subjects were covered by a combat jacket and blanket, respectively, to ensure adequate warmth. Frostnip may occur when the skin temperature reach -10 ℃ to -15 ℃ [56]. The cold exposure was terminated once it happened. In our simulation, we therefore assume that the core and mean skin temperature of the whole body were 37.1 ℃ and 31 ℃, respectively, and remained constant throughout the experiment [51]. This assumption is based on the fact that the surface area of a finger's middle segment is very small in comparison to the whole body and should therefore only have a negligible effect on the overall average. As the authors did not specify which specific finger was used in their experiments, we simulated the middle segments of all possible fingers (Fig. 3 and Fig. 4). The thumb was omitted as it does not have a middle segment. The wind speed for all other hand segments was assumed to be 0.05 m/s, and the corresponding convective heat transfer coefficients were obtained from the literature [40].

Clearly, the temperature change over time does not differ much between the different fingers. In Scenario 1, the largest differences between the experimental data and the numerical prediction of any finger segment's skin temperature are around 6 ℃ after 0.1 min. As time passes, this difference continually decreases and never exceeds 1.5 ℃ by the end of the experiment. In Scenario 2, the maximal temperature difference is around 3.5 ℃ and occurs at a time point of 0.15 min. Here, the differences remain below 1.1 ℃ by the end of the experiment. One possible reason for the relatively large initial discrepancies between the predicted and experimental tem-

peratures is that the experimental temperature was taken at a single point (i.e., the very center of the middle digit's dorsal), whereas our numerical simulation results were the area-weighted average temperature of the entire middle segment. Another reason may be related to the accuracy of the thermocouples (± 0.1 ℃) used in the experiment. Besides, in the experiment, the air temperature was measured a few millimeter to the test finger, and it differed from the temperature measured at the site of the finger by ± 0.5 ℃. Despite those discrepancies in the absolute values, the model is in good agreement with the experimental data and reproduces the observed temperature dynamics fairly well, thus showing its validity in those extreme cold scenarios. It can be concluded that by taking into consideration more realistic representations of the anatomy, geometry, physiology, and thermo-physical characteristics, our model could yield a better fit with the experimental data.

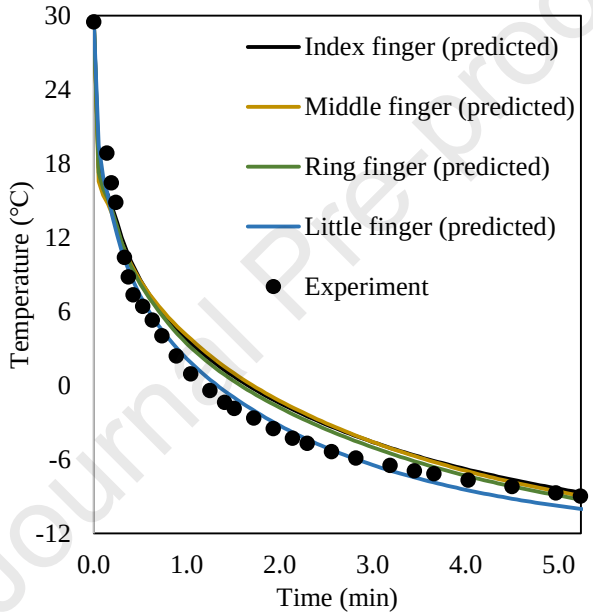

Fig. 3. Comparing the modeled change in skin temperature over time for Scenario 1 (-26 ℃ air temperature and 5 m/s wind speed) with experimental data from Wilson and Goldman [56].

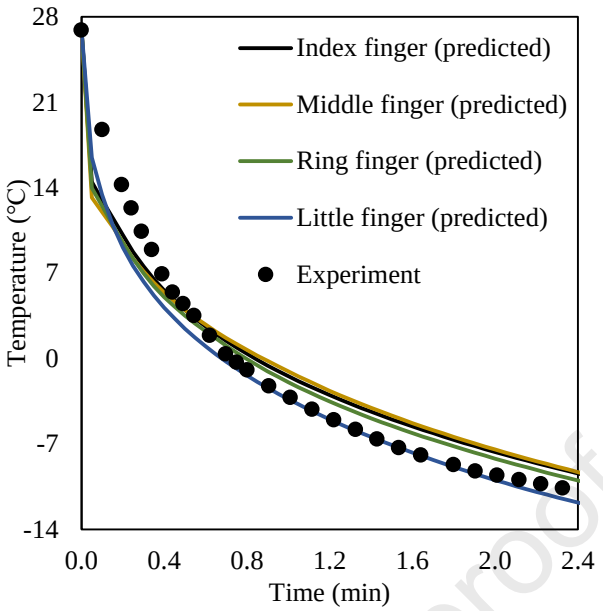

Fig. 4. Comparing the modeled change in skin temperature for Scenario 2 (-15°C air temperature and 10 m/s wind speed) with experimental data from Wilson and Goldman [56].

3.2 Model validation for Scenario 3

For scenario 3, the left hand was enclosed in a small climate chamber while the subject was inside a larger climate chamber with a temperature of 21 - 23 ℃. The air in the small climate chamber was slowly circulated at the speed below 0.4 m/s, while the temperature was controlled at 0 °C [57]. In the experiment, the temperatures of the index finger's tip, middle segment, and root, as well as the temperatures at the center of the palm and dorsal were measured. Each subject wore a T-shirt and long trousers to ensure adequate warmth. In the model, core and mean skin temperatures were assumed to be 37.1 ℃ and 31 ℃, respectively [51]. The wind speed at the hand was set to 0.4 m/s.

Generally, the modeled and measured skin temperature changes over time agree reasonably well (Fig. 5). The maximal differences between the predicted and experimental temperatures were observed at the palm and dorsal segments with about 2.68 ℃ and 1.45 ℃, respectively. At the index fingertip, middle segment, and root, the differences are below 1.5 ℃. As above, we ascribe these larger differences at the palm and dorsal to differences in methods obtaining the modeled versus the experimental values. While the experimental values represent spot measurements, the modeled values are area-weighted averages. If we consider possible errors resulting from the experimental measurement methods and those due to sensor precision (±0.2 ℃), the observed differences between the 3D model and the experiment are decent. Generally, it can be concluded that the 3D thermoregulation model can accurately predict the skin temperature at different segments in Scenario 3.

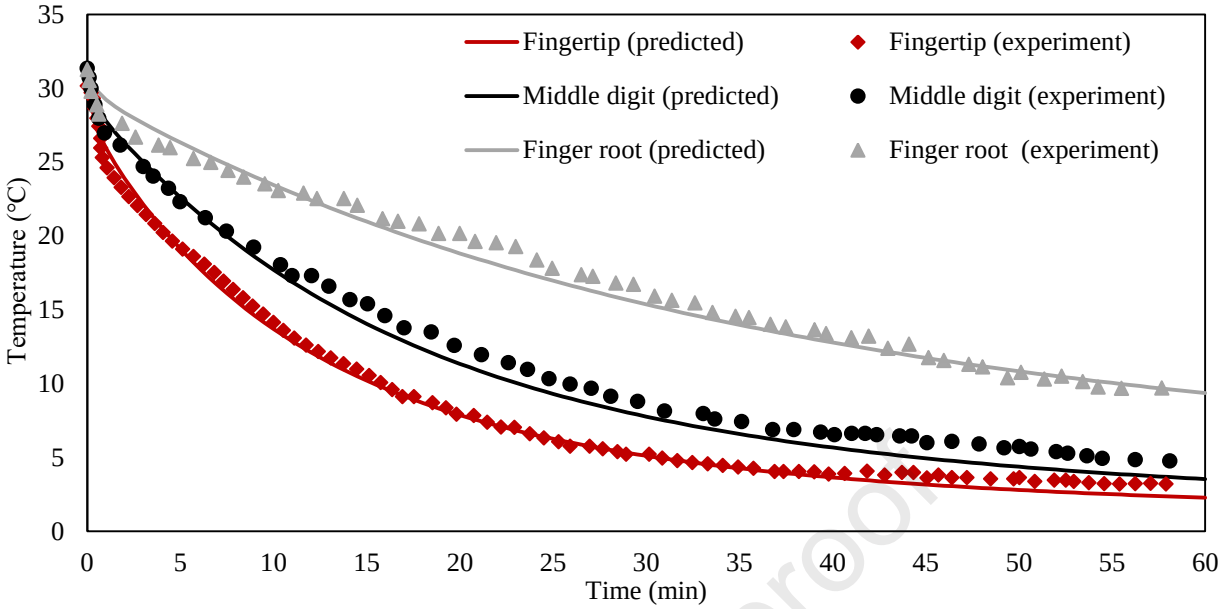

(a)

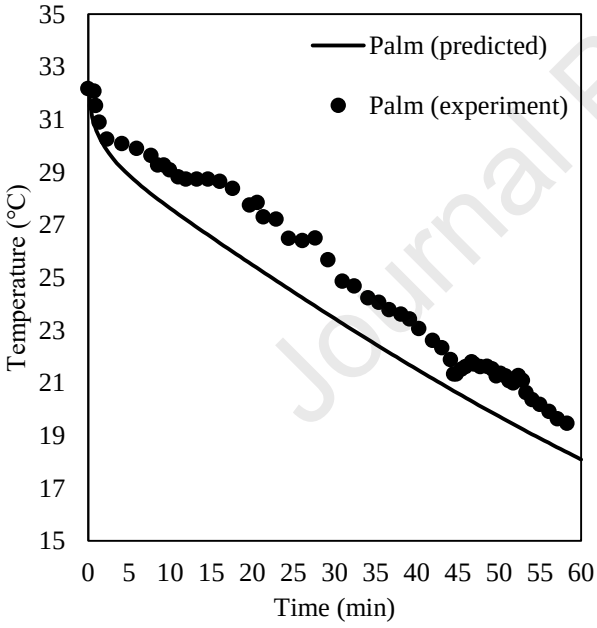

(b)

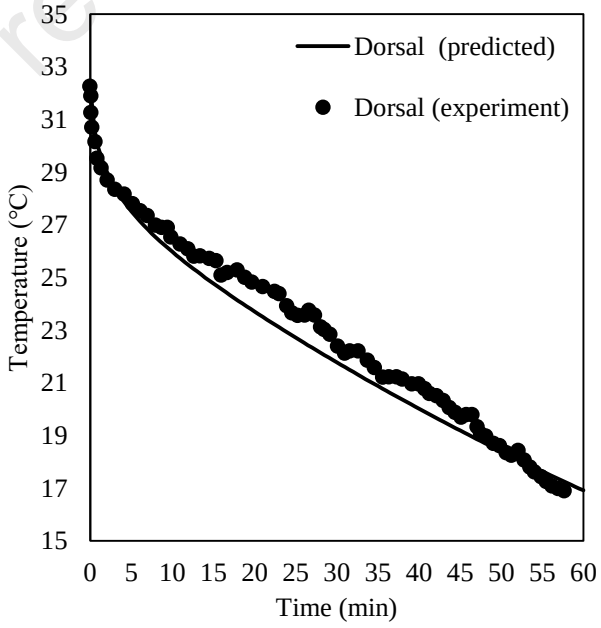

(c)

Fig. 5. Comparison between modeled and experimental (from [57]) skin temperature change for Scenario 3 (0 ℃ and 0.4 m/s wind speed) for (a) index finger, (b) palm, and (c) dorsal.

We also compared our model results with those predicted by the model developed by Shitzer et al. [37] (Fig. 6). In Shitzer et al.'s model, only the middle finger was modeled, considering effects of heat conduction, metabolic heat generation, heat transport by blood perfusion, heat exchange between the tissue and large blood vessels, and arterio-venous heat exchange. They divided the tissue into four concentric layers: core, muscle, fat, and skin. The heat transfer

coefficients, h_c, they used for the bare finger were 7.02 W/m^2·K and 9.46 W/m^2·K for the circumferential surface and the fingertip, respectively; in our model, we assigned those same h_c values to the middle segment of the middle finger and its fingertip, respectively. Using a previously developed model for calculating h_c [40], we were able to derive the wind speed that corresponds to the above h_c values: about 0.15 m/s. Based on this result, we used the model from [40] to calculate h_c for the remaining hand segments. Commensurate with the experimental conditions in [37] we again assumed the core and mean skin temperatures of the whole body to be 37.1 ℃ and 31 ℃, respectively [51].

Both models perform very similarly for predicting the change in skin temperature of the middle finger's tip (Fig. 6). The predictions by our model are slightly higher (1.0 °C) than those from Shitzer et al.'s model. The difference may be due to different finger geometries modeled. While we modeled the realistic hand geometry, Shitzer et al. model a singer finger. In still air condition, the thermal boundary layer between fingers may merge, and influence the convective heat transfer coefficient thus the skin temperature of each finger. Therefore, a whole hand model may better represent the heat transfer of the hand than a single finger model.

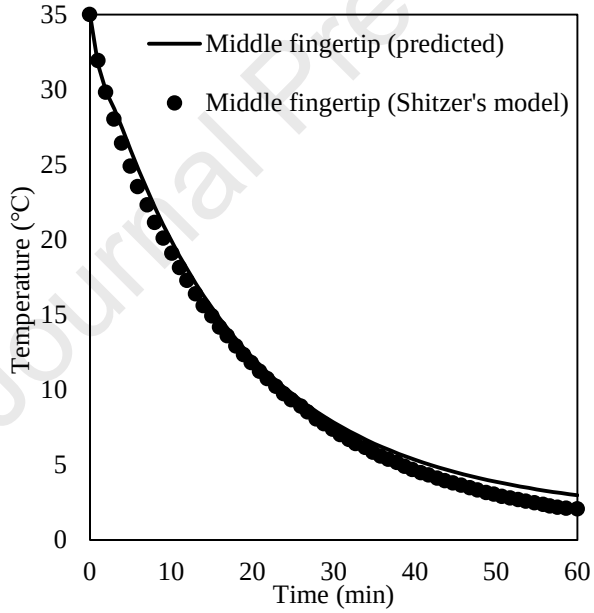

Fig. 6. Comparison with Shitzer's model of skin temperature profile under 0 ℃ temperature.

3.3 Model validation for Scenario 4

To validate the model for the "slightly cold" Scenario 4 (14 °C with 1.5 m/s wind), we compared our simulation results to experimental skin temperature data from Wang et al. [58] for the ring finger (Fig. 7). During the experiments, the subjects wore leotards and socks with an insulation value of 0.32 clo and sat in a thermally neutral environment that was kept at 28.4 ℃. The subject's left hand was cooled at an air temperature of 14 ℃ for a period of 20 min. The

cool air was supplied to the hand through an air sleeve covering the whole hand. The experiment consisted of spot measurements of the skin temperature of the ring finger's middle segment dorsal side and of the left hand dorsal plus continuous measurements of the core temperature. For the model, we assumed a mean skin temperature of 34 ℃ and a core temperature of 37.04 ℃ based on their experimental data. The wind speed was assumed to be 1.5 m/s [59, 60]. The simulated skin temperatures and temporal dynamics are again in good agreement with the experimental data (Fig. 7). The largest differences between the predicted and experimental skin temperatures are 1.48 ℃ and 0.82 ℃ for the ring finger and dorsal, respectively. This could be due to the different approaches used to obtain the skin temperature: while the skin temperatures in the experiments correspond to a single point measurement, the modeled skin temperature corresponds to an area-weighted average. Another reason for the discrepancy could be the error margin of the thermocouple (±0.2 ℃) used to measure skin temperatures. Nevertheless, the model agrees fairly well with the observations.

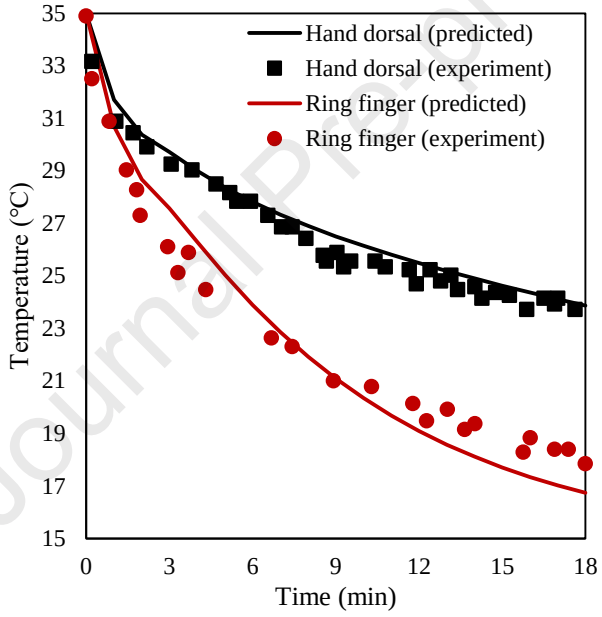

Fig. 7. Comparing model predictions of the ring finger's middle segment dorsal and hand dorsal temperatures to experimental data from Wang et al. [58] for Scenario 4 (14 ℃ and 1.5 m/s wind).

3.4 Model validation for CIVD

We also compared the model predictions of a CIVD event in the thumb to experimental data from [61] (Fig. 8). During the experiment, the bare hand was exposed for 60 min to a cold environment at an air temperature of 0 ℃ and with still wind. The temperature of the hand was measured by an infrared camera. In our model, we again assumed a core and average skin temperature of the whole body of 37.1 ℃ and 31 ℃, respectively [51]. The heat transfer coefficients were taken from [61]. The onset times of two CIVD events were set to t_1= 22 min and t_2=39 min.

The peak blood flow rates of two CIVD events were assumed to be 0.001 s^{-1} and 0.0009 s^{-1}, respectively. The maximum discrepancies between modeled and observed skin temperatures were about 1.66 ℃ and 1.20 ℃ at the beginning and end of the second CIVD event, respectively. These differences are mainly due to the smaller magnitude of the second CIVD compared to the first event. However, considering the large variability of the magnitude, onset time, and peak temperature of CIVD between different individuals, the observed difference between the model and experiment is relatively small and can be considered as acceptable. We therefore conclude that our model can simulate the characteristics of CIVD with sufficient accuracy.

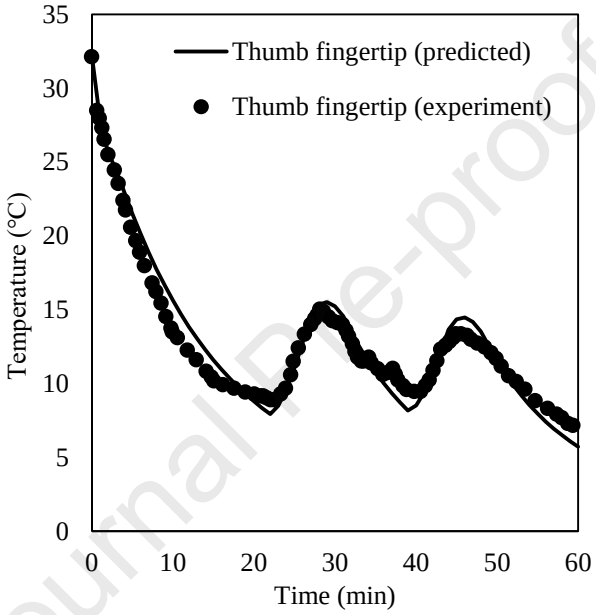

Fig. 8. Comparison of the model results of the skin temperature at the thumb's fingertip with experimental data from [61] during several CIVD events (at an ambient temperature of 0 ℃ with still air).

3.5 Model validation for the gloved hand

Fig. 9 shows a comparison between the present 3D model and experimental data from reference [62] of the average skin temperature at the middle and little fingertip with the glove. During the experiment, subjects wore a multilayer uniform, commonly used by the military to keep the body warm in winter, and remain seated in a chamber with an ambient air temperature of -6.7 ℃ and a wind speed of 1.1 m/s. The glove used to shield the hand from the cold was a light-duty type (thickness of 4.56 mm) with a leather shell and polyester inner layer [37]. The thermal insulation of the glove was 0.124 $m^2 \cdot K/W$ (0.8 clo), which was measured using an aluminum hand manikin. The temperature measurements were taken at the lateral nail bed of the middle and little fingers. The experiment was ended if the skin surface temperature dropped to 5 ℃.

We again assumed a core temperature and average skin temperature of the whole body of 37.1 ℃ and 31 ℃, respectively [51]. CIVD was assumed to occur at the little fingertip 27 min into the exposure according to the experimental data, and the peak blood flow rate was assumed to be 0.0009 s^{-1}. The glove layer was simulated by adding the thermal insulation value of the glove to the total heat transfer coefficient of the outer hand layer (Eq. 18 - Eq. 21). We adopted the exact same insulation for all local segments since no locational insulation value available from the experiment.

$$I_{air} = 1/(h_c + h_r) \quad \text{Eq. 18}$$

where I_{air} (m^2·K/W) is the thermal insulation afforded to the naked hand by air and h_r (W/(m^2·K)) is the radiative heat transfer coefficient. For a gloved hand, the surface area for heat transfer is increased due to the thickness of the glove layer. This was taken into consideration by using a glove area factor:

$$f_{glove} = A_{glove}/A_{hand} \quad \text{Eq. 19}$$

with A_{glove} (m^2) and A_{hand} (m^2) the surface areas of the gloved and naked hand, respectively. A_{hand} was calculated based on the geometrical model of the hand and A_{glove} was obtained using a simple scaling factor to grow the hand model to account for the thickness added by the glove. While this approach neglects possible air gaps between the inner side of the glove and the hand skin, the associated error should be negligible considering the tight fit of the glove.

The thermal insulation for the gloved hand due to the boundary air is

$$I_{air,glove} = I_{air}/f_{glove} \quad \text{Eq. 20}$$

while the total thermal insulation (glove plus surrounding air) is:

$$I_{total} = I_{glove} + I_{air,glove} \quad \text{Eq. 21}$$

It can be seen from Fig. 9 that the predicted change in skin temperature is in good agreement with the experimental data with differences remaining below 0.74 ℃. This shows that our 3D thermoregulation model can predict the skin temperature of a gloved finger with sufficient accuracy.

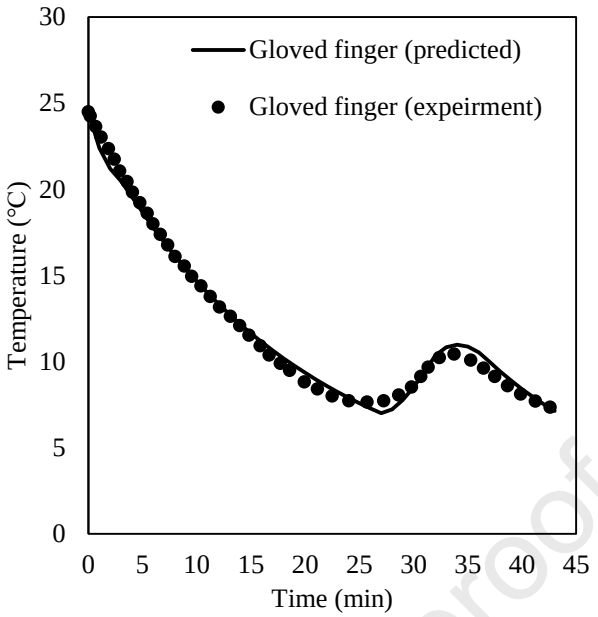

Fig. 9. Comparison of predicted and experimental averaged skin temperature (using data from [62]) of the gloved middle and little fingertips.

3.6 Temperature profiles of the 3D hand under various environmental conditions

Previous sections have shown that the present 3D thermoregulation model can accurately predict the temporal change of hand skin temperature in a wide range of cold environments. A strong point of this model is that it can predict and visualize the temperature distribution and changes over time for both the whole hand and individual segments (Fig. 10).

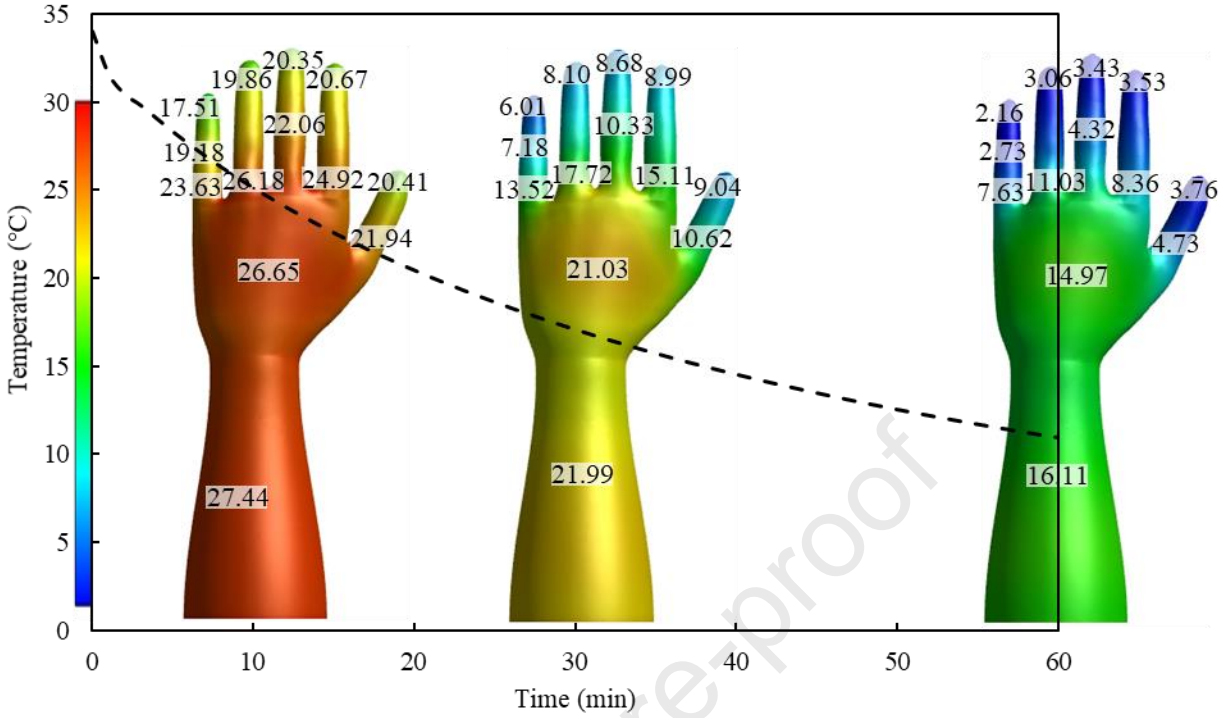

Fig. 10. Example simulations to demonstrate the model's capabilities to predict the skin temperature distribution and change over time in individual hand segments. Ambient conditions: 0 ℃ air temperature and 0.05 m/s wind speed. The dotted line shows the area-weighted average temperature of the whole hand over time and the individual numbers correspond to the area-weighted averages of the individual hand segments. Only the dorsal side is shown since the temperature difference between the palm and dorsal segments is typically quite small (below 0.87 ℃ for wind speeds ranging from 0.05 m/s to 2.0 m/s and air temperatures range from -10 ℃ to 10 ℃).

We also investigated the effect of air flow to the dorsal side of the hand since the dorsal segments are most frequently exposed to wind when working. For this simulation, we assumed that the subject wore adequate clothing to keep the body sufficiently warm with only the hands exposed to the cold environment. We therefore assumed the body core temperature and average skin temperature of the whole body to be 37.1 ℃ and 34 ℃, respectively [51]. The initial temperatures of the soft tissue and the bone core were also both set to 34 ℃ [45].

We simulate the air temperature from -10 ℃ to 10 ℃ to investigate the effect of air temperature on the thermal response of the hand. When exposing the hand to different air temperatures, the skin temperature decreases with time and asymptotically approaches the ambient air temperature (Fig. 11a). The cooling rate of the hands increases with decreasing air temperature. The difference in hand skin temperature, ΔT_{hand} increases exponentially with time and reaches a maximum at the end of the exposure, with ΔT_{hand} = 6.87 ℃ when going from 0 ℃ to -10 ℃ air temperature and ΔT_{hand} = 7.32 ℃ when going from 10 ℃ to 0 ℃ air temperature.

Another interesting result of this simulation was the major differences among the skin temperatures at different hand segments (Fig. 11b-d). Generally, the forearm, palm, and dorsal segments have higher skin temperatures and the tip of the little finger has the lowest skin tem-

perature. Furthermore, the temperature differences among different hand segments increase with decreasing air temperature. At 10 ℃, the skin temperature of the little fingertips is 9.93 ℃ below the skin temperature of the hand's dorsal side. In the 0 ℃ and -10 ℃ environments, this difference increases to 12.81 ℃ and 16.14 ℃, respectively. This indicates what in very cold environments, the palm and dorsal segments of the hand may still feel comfortably warm or only slightly cold, whereas the fingers may have already lost much dexterity or even suffered a cold injury. Thus, when designing protective gloves for cold environments, more attention needs to be paid to the prevention of heat loss from the fingertips. The fact that the lowest temperature is seen at the tip of the little finger would make this hand segment a prime candidate for use as a critical indicator when trying to predict and evaluate the danger of cold injury and loss of dexterity.

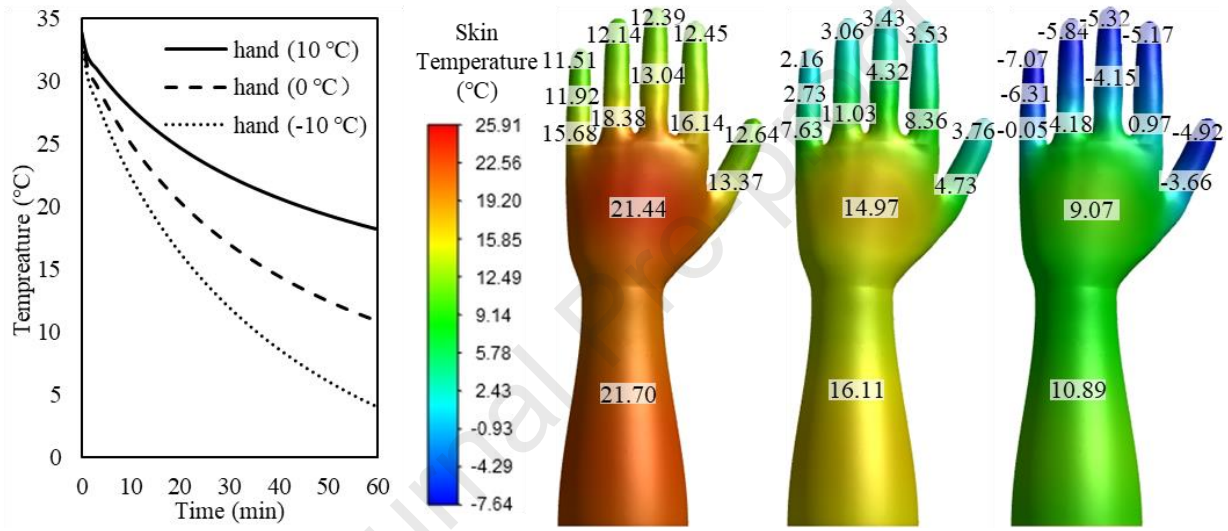

Fig. 11. (a) Change in hand skin temperature over time at 0.05 m/s wind speed, (b) skin temperature distribution after a 60 min exposure to 0.05 m/s wind speed and an ambient temperature of 10 ℃, (c) 0 ℃, and (d) -10 ℃.

We also examined the change in hand skin temperature as a function of wind speed (Fig. 12a). A wind speed range from 0.05 m/s to 2.0 m/s was selected to utilize a series of validated convective heat transfer coefficients of different hand segments with real hand geometry [40]. As expected, the temperature of the hand decreases with increasing wind speed. More specifically, when the wind speed is increased from 0.05 m/s to 1.0 m/s, the average skin temperature has decreased by 6.57 °C after 60 min exposure while a further increase in wind speed from 1.0 m/s to 2.0 m/s leads to a much smaller decrease in the hand skin temperature of just 1.49 ℃ after 60 min exposure. Wind chill significantly affects heat loss during cold exposure although the increase in the rate of cooling slows down for higher wind velocities. When the wind speed is 0.05 m/s, the skin temperature of the hand decreases almost linearly with time. For a wind speed of 1.0 m/s, the hand skin temperature shows a marked decrease during the initial stage of exposure and then decreases more slowly as it approaches the ambient temperature. Wind can increase the convective heat transfer coefficient, thus leading to enhanced heat loss. Higher wind speed leads

to a higher cooling rate during the initial stage of exposure, after which the skin tends to cool down more slowly than the still air scenario while tending toward the ambient temperature. However, wind speed has no effect on the final temperature that a hand will reach after very long exposure since the skin temperature cannot decrease below the ambient temperature.

During cold exposure, the higher the wind speed the more quickly the initial drop in skin temperature in each hand segment (Fig. 12b-d). As above (Fig. 11) we again find large differences between individual segments, with the tip of the little finger always showing the lowest skin temperature. These differences between segments decrease with increasing wind speed. For 0.05 m/s, the skin temperature of the little fingertip is 12.81 ℃ below the temperature of the hand dorsal segment. This difference decreases to 6.82 ℃ and 4.61 ℃ at wind speeds of 1.0 m/s and 2.0 m/s, respectively.

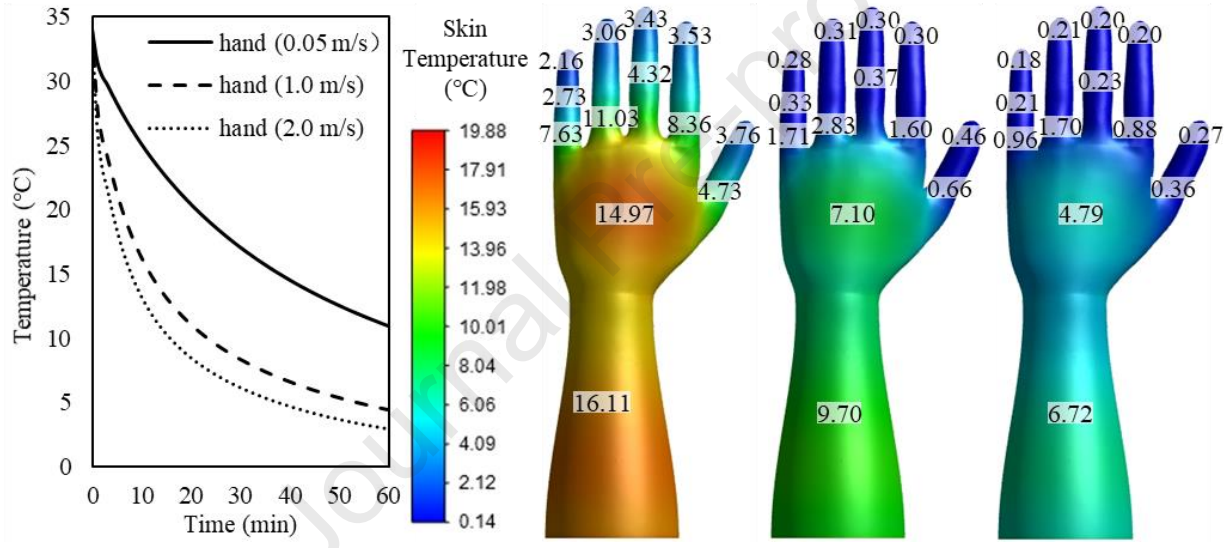

Fig. 12. (a) Change in overall hand skin temperature over time for at 0 °C air temperature, (b) skin temperature distribution after a 60 min exposure to 0 °C air temperature at a wind speed of 0.05 m/s, (c) 1.0 m/s, and (d) 2.0 m/s.

4 Conclusions and future perspective

In this study, a multi-segment 3D hand-specific thermoregulation model was developed for predicting and visualizing the spatial and temporal temperature profiles of a hand exposed to various cold environments. The 3D model possesses the following specific features:

(1) It yields an enhanced understanding of thermal responses of the hand by employing realistic hand anthropometry, anatomy, as well as thermo-physical and physiological properties.

(2) The multi-segment approach will allow to account for the heterogeneity of physiological and thermo-physical properties of the hand, distinguish thermal responses

between hand segments, and identify particularly vulnerable parts of the hand with regard to cold injury.

(3) The hand-specific thermoregulation model is fully 3D and transient, thus has an innovative benefit over current one-dimensional (1D), two-dimensional (2D), and single-finger thermoregulation with regard to visualizing the temporal and spatial skin temperature over the hand.

(4) It can simulate the effect of gloves, changes in blood flow, and CIVD. Moreover, the model can accurately predict the skin temperature under a wide range of ambient conditions and air temperatures from slightly cold to extremely chilling environments. It is thus a reliable, safe, and cost-effective tool to predict the hand skin temperature for various indoor and outdoor environments ranging from cool to extreme cold.

The model developed in this study provides a significant advancement of the state-of-the-art in hand thermoregulation modeling. It addresses several critical issues associated with understandings of the thermal interaction between the hand and the cold built environment and furthers the current knowledge of the underlying mechanisms of hand thermoregulation. The outcomes of this study facilitate the formulation of improved guidelines for glove design and engineering, which will ultimately improve work efficiency, safety, and health for various occupations.

Presently, very little is known about the thermoregulatory mechanisms of the hand during cold exposure such as CIVD, for which quantitative studies are sparse, often producing inconsistent results in terms of onset time, response magnitude, and duration. Future research should focus on exploring the CIVD mechanisms and derive mathematical expressions that quantitatively describe and explain CIVD. Another critical point that future work should focus on is to determine realistic tissue properties of each hand segment. Thermoregulation models require tissue density, thermal conductivity, specific heat capacity, blood perfusion, and metabolic heat production. However, the composition of the hand is complex, and the data about the distribution and percentage of bone, muscle, tendon, fat, and skin is limited. Future research should focus on identifying these factors and facilitating determining the composition of each hand section with more accuracy.

Acknowledgments

Fire Prevention and Safety (FP&S) Research and Development (R&D) Grants, which are part of the Assistance to Firefighters Grants (AFG) with funding from the U.S. Department of Homeland Security (DHS), Federal Emergency Management Agency (FEMA) is thanked for its

financial support (project number EMW-2018-FP-00649). FP&S aims to reduce firefighter fatal and nonfatal injuries and improve firefighter safety, health and wellness.

Dr. Xinwei Wang from Iowa State University is thanked for his suggestions and editing to this manuscript.

References

[1] H. Anttonen, A. Pekkarinen, and J. Niskanen, "Safety at work in cold environments and prevention of cold stress," *Industrial health,* vol. 47, no. 3, pp. 254-261, 2009, doi: https://doi.org/10.2486/indhealth.47.254.

[2] X. Chen, P. Xue, L. Gao, J. Du, and J. Liu, "Physiological and thermal response to real-life transient conditions during winter in severe cold area," *Building and Environment,* vol. 157, pp. 284-296, 2019, doi: 10.1016/j.buildenv.2019.04.004.

[3] R. Heus, H. A. Daanen, and G. Havenith, "Physiological criteria for functioning of hands in the cold: a review," *Applied Ergonomics,* vol. 26, no. 1, pp. 5-13, Feb 1995, doi: 10.1016/0003-6870(94)00004-i.

[4] W. L. Chen, Y. C. Shih, and C. F. Chi, "Hand and finger dexterity as a function of skin temperature, EMG, and ambient condition," *Human factors,* vol. 52, no. 3, pp. 426-40, Jun 2010, doi: 10.1177/0018720810376514.

[5] C. Zimmermann, W. H. Uedelhoven, B. Kurz, and K. J. Glitz, "Thermal comfort range of a military cold protection glove: database by thermophysiological simulation," *European journal of applied physiology,* vol. 104, no. 2, pp. 229-36, Sep 2008, doi: 10.1007/s00421-007-0660-z.

[6] J. M. Lockhart, H. O. Kiess, and T. J. Clegg, "Effect of rate and level of lowered finger surface temperature on manual performance," *Journal of Applied Psychology,* vol. 60, no. 1, pp. 106-113, 1975, doi: 10.1037/h0076269.

[7] H. A. M. Daanen, "Manual Performance Deterioration in the Cold Estimated Using the Wind Chill Equivalent Temperature," *Industrial Health,* vol. 47, no. 3, pp. 262-270, 2009, doi: https://doi.org/10.2486/indhealth.47.262.

[8] J. Hunter, E. Kerr, and M. Whillans, "The relation between joint stiffness upon exposure to cold and the characteristics of synovial fluid," *Canadian Journal of Medical Sciences,* vol. 30, no. 5, pp. 367-377, 1952.

[9] R. E. Schiefer, R. Kok, M. I. Lewis, and G. B. Meese, "Finger Skin Temperature and Manual Dexterity - Some Inter-Group Differences," (in English), *Applied Ergonomics,* vol. 15, no. 2, pp. 135-141, 1984, doi: Doi 10.1016/0003-6870(84)90291-6.

[10] W. F. Fox, "Human Performance in the Cold," *Human factors,* vol. 9, no. 3, pp. 203-220, 1967, doi: https://doi.org/10.1177/001872086700900302.

[11] R. S. Goonetilleke and E. R. Hoffmann, "Hand-skin temperature and tracking performance," *International Journal of Industrial Ergonomics,* vol. 39, no. 4, pp. 590-595, 2009, doi: 10.1016/j.ergon.2008.01.009.

[12] G. Havenith, R. Heus, and H. A. Daanen, "The hand in the cold, performance and risk," *Arctic Medical Research,* vol. 54 Suppl 2, pp. 37-47, 1995. [Online]. Available: https://www.ncbi.nlm.nih.gov/pubmed/8900831.

[13] X. Xu, P. Tikuisis, R. Gonzalez, and G. Giesbrecht, "Thermoregulatory model for prediction of long-term cold exposure," *Computers in biology and medicine,* vol. 35, no. 4, pp. 287-298, 2005.

[14] W. R. Santee, A. W. Potter, and K. E. Friedl, "Talk to the hand: U.S. army biophysical testing," *Mil Med,* vol. 182, no. 7, pp. e1702-e1705, Jul 2017, doi: 10.7205/MILMED-D-16-00156.

[15] J. A. Stolwijk and J. D. Hardy, "Control of body temperature," *Comprehensive Physiology,* pp. 45-68, 2010, doi: https://doi.org/10.1002/cphy.cp090104.

[16] R. E. Forster, B. G. Ferris, and R. Day, "The relationship between total heat exchange and blood flow in the hand at various ambient temperatures," *American Journal of Physiology-Legacy Content,* vol. 146, no. 4, pp. 600-609, 1946.

[17] N. A. S. Taylor, C. Machado-Moreira, A. v. d. Heuvel, J. Caldwell, E. A. Taylor, and M. J. Tipton, "The roles of hands and feet in temperature regulation in hot and cold environments," in *The 13th International Conference on Environmental Ergonomics*, Boston, USA, 2009.

[18] T. Nagasaka, M. Cabanac, K. Hirata, and T. Nunomura, "Control of local heat gain by vasomotor response of the hand," *Journal of Applied Physiology,* vol. 63, no. 4, pp. 1335-1338, 1987, doi: 10.1152/jappl.1987.63.4.1335.

[19] R. W. Wilkins, J. Doupe, and H. W. Newman, "The rate of blood flow in normal fingers," *Clinical Science,* vol. 3, pp. 403-411, 1938.

[20] A. D. Flouris, D. A. Westwood, I. B. Mekjavic, and S. S. Cheung, "Effect of body temperature on cold induced vasodilation," *European journal of applied physiology,* vol. 104, no. 3, pp. 491-499, Oct 2008, doi: 10.1007/s00421-008-0798-3.

[21] H. A. Daanen, "Finger cold-induced vasodilation: a review," *European journal of applied physiology,* vol. 89, no. 5, pp. 411-426, 2003, doi: 10.1007/s00421-003-0818-2.

[22] A. D. Flouris and S. S. Cheung, "Influence of thermal balance on cold-induced vasodilation," *Journal of Applied Physiology,* vol. 106, no. 4, pp. 1264-1271, Apr 2009, doi: 10.1152/japplphysiol.91426.2008.

[23] C. O'Brien, "Reproducibility of the cold-induced vasodilation response in the human finger," *Journal of Applied Physiology,* vol. 98, no. 4, pp. 1334-1340, Apr 2005, doi: 10.1152/japplphysiol.00859.2004.

[24] M. Guiatni and A. Kheddar, "Theoretical and experimental study of a heat transfer model for thermal feedback in virtual environments," in *2008 IEEE/RSJ International Conference on Intelligent Robots and Systems*, 2008: IEEE, pp. 2996-3001.

[25] H.-N. Ho and L. A. Jones, "Modeling the thermal responses of the skin surface during hand-object interactions," *Journal of Biomechanical Engineering,* vol. 130, no. 2, 2008.

[26] E. Ungar and K. Stroud, "A new approach to defining human touch temperature standards," in *40th International Conference on Environmental Systems*, 2010, p. 6310.

[27] K. Katić, R. Li, and W. Zeiler, "Thermophysiological models and their applications: A review," *Building and Environment,* vol. 106, pp. 286-300, 2016, doi: 10.1016/j.buildenv.2016.06.031.

[28] M. Fu, W. Weng, W. Chen, and N. Luo, "Review on modeling heat transfer and thermoregulatory responses in human body," *Journal of thermal biology,* vol. 62, no. Pt B, pp. 189-200, 2016, doi: 10.1016/j.jtherbio.2016.06.018.

[29] K. Katic, R. Li, B. Kingma, and W. Zeiler, "Modelling hand skin temperature in relation to body composition," *Journal of thermal biology,* vol. 69, pp. 139-148, Oct 2017, doi: 10.1016/j.jtherbio.2017.07.003.

[30] D. Fiala, G. Havenith, P. Brode, B. Kampmann, and G. Jendritzky, "UTCI-Fiala multi-node model of human heat transfer and temperature regulation," *International journal of biometeorology,* vol. 56, no. 3, pp. 429-441, May 2012, doi: 10.1007/s00484-011-0424-7.

[31] A. Dixit and U. Gade, "A case study on human bio-heat transfer and thermal comfort within CFD," *Building and Environment,* vol. 94, pp. 122-130, 2015, doi: 10.1016/j.buildenv.2015.07.016.

[32] M. S. Ferreira and J. I. Yanagihara, "A heat transfer model of the human upper limbs," *International Communications in Heat and Mass Transfer,* vol. 39, no. 2, pp. 196-203, 2012, doi: 10.1016/j.icheatmasstransfer.2011.12.004.
[33] A. Fallahi, M. R. Salimpour, and E. Shirani, "Analytical expressions for estimating endurance time and glove thermal resistance related to human finger in cold conditions," *Journal of thermal biology,* vol. 69, pp. 334-340, Oct 2017, doi: 10.1016/j.jtherbio.2017.09.006.
[34] A. Fallahi, M. R. Salimpour, and E. Shirani, "A 3D thermal model to analyze the temperature changes of digits during cold stress and predict the danger of frostbite in human fingers," *Journal of thermal biology,* vol. 65, pp. 153-160, Apr 2017, doi: 10.1016/j.jtherbio.2017.03.001.
[35] Y. He, H. Liu, R. Himeno, J. Sunaga, N. Kakusho, and H. Yokota, "Finite element analysis of blood flow and heat transfer in an image-based human finger," *Computers in biology and medicine,* vol. 38, no. 5, pp. 555-562, May 2008, doi: 10.1016/j.compbiomed.2008.02.002.
[36] A. Shitzer, L. A. Stroschein, R. R. Gonzalez, and K. B. Pandolf, "Lumped-parameter tissue temperature-blood perfusion model of a cold-stressed fingertip," *Journal of Applied Physiology,* vol. 80, no. 5, pp. 1829-1834, 1996, doi: 10.1152/jappl.1996.80.5.1829.
[37] A. Shitzer, L. A. Stroschein, P. Vital, R. R. Gonzalez, and K. B. Pandolf, "Numerical analysis of an extremity in a cold environment including countercurrent arterio-venous heat exchange," *Journal of biomechanical engineering,* vol. 119, no. 2, pp. 179-186, May 1997, doi: 10.1115/1.2796078.
[38] W. Karaki, N. Ghaddar, K. Ghali, K. Kuklane, I. Holmér, and L. Vanggaard, "Human thermal response with improved AVA modeling of the digits," *International Journal of Thermal Sciences,* vol. 67, pp. 41-52, 2013, doi: 10.1016/j.ijthermalsci.2012.12.010.
[39] H. Shao, Y. He, and L. Mu, "Numerical analysis of dynamic temperature in response to different levels of reactive hyperaemia in a three-dimensional image-based hand model," *Computer methods in biomechanics and biomedical engineering,* vol. 17, no. 8, pp. 865-874, 2014, doi: 10.1080/10255842.2012.723698.
[40] M. Zhang, R. Li, Y. Wu, L. Wang, G. Song, and J. Li, "Numerical study of the convective heat transfer coefficient of the hand and the effect of wind," *Building and Environment,* vol. 188, 2021, doi: 10.1016/j.buildenv.2020.107482.
[41] X. Xu and P. Tikuisis, "Thermoregulatory modeling for cold stress," *Comprehensive Physiology,* vol. 4, no. 3, pp. 1057-1081, 2014, doi: 10.1002/cphy.c130047.
[42] Z. Kang, F. Wang, and Udayraj, "An advanced three-dimensional thermoregulation model of the human body: Development and validation," *International Communications in Heat and Mass Transfer,* vol. 107, pp. 34-43, 2019, doi: 10.1016/j.icheatmasstransfer.2019.05.006.
[43] L. Ding, "The study of thermal protection of EVA space glove," Ph.D., Human-machine and environmental engineering, BeiHang University, Beijing, China, 2000.
[44] J. Werner and P. Webb, "A six-cylinder model of for general use on human thermoregulation personal computers," *The Annals of physiological anthropology,* vol. 12, no. 3, pp. 123-134, 1993, doi: https://doi.org/10.2114/ahs1983.12.123.
[45] P. Tikuisis, "Finger cooling during cold air exposure," (in English), *Bulletin of the American Meteorological Society,* vol. 85, no. 5, pp. 717-723, May 2004, doi: 10.1175/Bams-85-5-717.
[46] X. Yuan, *Mathematical simulation of human body thermoregulation*. Beijing: Beihang University Press, 2005.
[47] R. J. Maughan, J. S. Watson, and J. Weir, "The relative proportions of fat, muscle and bone in the normal human forearm as determined by computed tomography," *Clinical science,* vol. 66, no. 6, pp. 683-689, 1984, doi: https://doi.org/10.1042/cs0660683.
[48] A. K. Dixon, D. J. Bowden, H. Ellis, and B. M. Logan, *Human Sectional Anatomy Atlas of Body Sections, CT and MRI Images - 4th Edition*. CRC Press, 2015.

[49] K. E. Cooper, O. G. Edholm, and R. F. Mottram, "The blood flow in skin and muscle of the human forearm," *The Journal of Physiology,* vol. 128, no. 2, pp. 258-267, 1955, doi: 10.1113/jphysiol.1955.sp005304.

[50] M. Edwards and A. C. Burton, "Correlation of Heat Output and Blood Flow in the Finger, Especially in Cold-Induced Vasodilation," (in English), *Journal of Applied Physiology,* vol. 15, no. 2, pp. 201-208, 1960, doi: https://doi.org/10.1152/jappl.1960.15.2.201.

[51] W. A. Lotens, "Simulation of hand cooling due to touching cold materials," *European journal of applied physiology and occupational physiology,* vol. 65, no. 1, pp. 59-65, 1992, doi: doi:10.1007/BF01466275.

[52] J. D. Coffman, "Total and nutritional blood flow in the finger," *Clinical science,* vol. 42, no. 3, pp. 243-250, 1972.

[53] K. Parsons, *Human thermal environments: the effects of hot, moderate, and cold environments on human health, comfort, and performance*. CRC press, 2014.

[54] S. S. Cheung, "Responses of the hands and feet to cold exposure," *Temperature (Austin),* vol. 2, no. 1, pp. 105-20, Jan-Mar 2015, doi: 10.1080/23328940.2015.1008890.

[55] A. Enander, "Perception of hand cooling during local cold air exposure at three different temperatures," *Ergonomics,* vol. 25, no. 5, pp. 351-61, May 1982, doi: 10.1080/00140138208925001.

[56] O. Wilson and R. F. Goldman, "Role of air temperature and wind in the time necessary for a finger to freeze," *Journal of Applied Physiology,* vol. 29, no. 5, pp. 658-664, Nov 1970, doi: 10.1152/jappl.1970.29.5.658.

[57] F. Chen, Z. Y. Liu, and I. Holmer, "Hand and finger skin temperatures in convective and contact cold exposure," *European journal of applied physiology and occupational physiology,* vol. 72, no. 4, pp. 372-379, 1996, doi: 10.1007/BF00599699.

[58] D. Wang, H. Zhang, E. Arens, and C. Huizenga, "Observations of upper-extremity skin temperature and corresponding overall-body thermal sensations and comfort," *Building and Environment,* vol. 42, no. 12, pp. 3933-3943, 2007, doi: 10.1016/j.buildenv.2006.06.035.

[59] C. Huizenga, H. Zhang, E. Arens, and D. Wang, "Skin and core temperature response to partial- and whole-body heating and cooling," *Journal of Thermal Biology,* vol. 29, no. 7-8, pp. 549-558, 2004, doi: 10.1016/j.jtherbio.2004.08.024.

[60] H. Zhang, "Human thermal sensation and comfort in transient and non-uniform thermal environments," Doctor of Philosophy, Architecture, University of California, Berkeley, 2003.

[61] A. Shitzer, S. Bellomo, L. A. Stroschein, R. R. Gonzalez, and K. B. Pandolf, "Simulation of a cold-stressed finger including the effects of wind, gloves, and cold-induced vasodilatation," *Journal of biomechanical engineering,* vol. 120, no. 3, pp. 389-394, Jun 1998, doi: 10.1115/1.2798006.

[62] W. R. Santee, T. L. Endrusick, and L. S. Pensotti, "Comparison of light duty gloves with natural and synthetic materials under wet and dry conditions," U.S. Army Rsch Inst of Env Med, 1990.

- A 3D multi-segment hand-specific thermoregulation model is developed.
- The model is a more realistic representation of the hand's anatomy and physiology.
- The model accounts for the hand's inhomogeneity by dividing it into 17 segments.
- Cold-induced vasodilation (CIVD) in fingers was simulated.
- The model predicts the spatial and temporal skin temperature accurately.

Declaration of Statement

The authors declare that they have no known competing financial or personal relationships with other people or organizations that could inappropriately influence (bias) the work reported in this paper.